Solvent-driven, self-assembled acid-responsive poly(ketalized serine)/siRNA complexes for RNA interference

Journal:	*Biomaterials Science*
Manuscript ID	BM-ART-09-2020-001478.R1
Article Type:	Paper
Date Submitted by the Author:	29-Sep-2020
Complete List of Authors:	Wong, Shirley; UC Irvine, Pharmaceutical Sciences Kemp, Jessica; UC Irvine Shim, Min Suk; Incheon National University, Division of Bioengineering Kwon, Young Jik; University of California, Irvine, Pharmaceutical Sciences, and Chemical Engineering & Materials Science

SCHOLARONE™
Manuscripts

Solvent-driven, self-assembled acid-responsive poly(ketalized serine)/siRNA complexes for RNA interference

Shirley Wong, [a] Jessica Kemp, [a] Min Suk Shim, [b] and Young Jik Kwon*[a,c,d,e]

Advances in bionanotechnology aim to develop smart nucleic acid delivery carriers with stimuli-responsive features to overcome challenges such as non-biodegradability, rapid clearance, immune response, and reaching intracellular targets. Peptide-based nanomaterials have become widely used in the field of gene and drug delivery due to their structural versatility and biomimetic properties. Particularly, polypeptide gene vectors that respond to biological stimuli, such as acidic intracellular environments, have promising utilities in mediating efficient endosomal escape and drug release. Unfortunately, synthesis strategies for efficient polymerization of acid-labile peptides has been limited due to conditions that fail to preserve acid-degradable functional groups. Stable urethane derivatives of acid-labile amino acid, ketalized serine (kSer), were synthesized and polymerized to high molecular weight under permissive conditions independent of elevated temperature, restrictive solvents, or inert atmosphere. A new formulation strategy utilizing solvent-driven self-assembly of poly(kSer) peptides with small interfering RNA (siRNA) was developed, and the resulting poly(kSer)/siRNA complexes were further cross-linked for reinforced stability under physiological conditions. The complexes were highly monodisperse and precisely spherical in morphology which has significant clinical implications in definitive biodistribution, cellular internalization, and intracellular trafficking patterns. Self-assembled, cross-linked poly(kSer)/siRNA complexes demonstrated efficient nucleic acid encapsulation, internalization, endosomal escape, and acid-triggered cargo release, which tackles multiple hurdles in siRNA delivery. The acid-responsive polypeptides and solvent-deriven self-assembly strategies demonstrated in this study could be applicable to developing other efficient and safe delivery systems for gene and drug delivery.

Introduction

Clinical use of short interfering RNA (siRNA) is gaining momentum due to their high specificity and potency of silencing genes that contribute to pathological disorders.[1,2] Consequently, RNA interference (RNAi) can be used to treat a number of diseases, including cancer, HIV infection, Parkinson's disease, and age-related macular degeneration.[3-6] In 2018 ONPATTRO™ was the first FDA-approved siRNA therapeutic used to treat polyneuropathy of hereditary transthyretin - mediated amyloidosis in adults,[4] and there are at least 30 RNAi therapies in clinical trials.[1] Clinical RNAi therapy still faces many

challenges, particularly in formulating carriers that efficiently encapsulate siRNA, enhance cellular uptake and endosomal escape, and successfully release therapeutic contents into the cytoplasm.[7, 8] The effectiveness of siRNA delivery is largely determined by the physicochemical properties of the engineered gene carriers, such as size, shape, and charge.[9] Meanwhile, these same characteristics that enhance siRNA delivery must be balanced to minimize potential toxicity.[10-12] For example, positively charged nanocarriers electrostatically interact with cell membranes and favor surface adhesion. However, they may cause cell membrane damage, hemolysis, platelet aggregation, and elicit an immune response.[13] Furthermore, macromolecules with high cationic density may actually impede cytoplasmic release of siRNA due to such strong ionic interactions.[14] Therefore, an effective strategy to optimize physicochemical properties of siRNA carriers is critical in achieving effective siRNA delivery while avoiding adverse effects.

Cationic peptides are promising siRNA delivery carriers due to their electrostatic interactions with nucleic acids, high biocompatibility, low toxicity, biodegradability, and versatile molecular arrangements. [15-17] The cationic peptides bear multiple amines available for ionic interactions with the siRNA phosphate backbone for direct complexation of the nucleic acid.[18] However high nitrogen to phosphate (N/P) ratios results in some of the aforementioned toxicity due to high surface

a. Department of Pharmaceutical Sciences, School of Pharmacy and Pharmaceutical Sciences, University of California, Irvine, CA 92697, USA
b. Division of Bioengineering, Incheon National University, Incheon 22012, Republic of Korea
c. Department of Chemical &Biomolecular Engineering, University of California, Irvine, CA 92697, USA
d. Department of Biomedical Engineering, University of California, Irvine, CA 92697, USA
e. Department of Molecular Biology & Biochemistry, University of California, Irvine, CA 92697, USA
* Corresponding author. E-mail: kwonyj@uci.edu

ARTICLE

charges.[19] On the contrary, lower N/P ratios often limit molecular interactions between the carriers and nucleic acids, and fail to efficiently encapsulate nucleic acids, especially short oligonucleotide chains with increased stiffness such as siRNA.[20, 21] These issues may be circumvented through chemical modifications that alleviate cationic density yet trigger siRNA release within specific cellular environments. It has been demonstrated that polymers and polypeptides with stimuli-responsive cationic side chains can achieve both efficient complexation and de-complexation of nucleic acids.[22, 23]

Another advantage to peptide-based materials is the capacity to specifically engineer for self-assembly in distinct environments.[24] Considerable advances have been made using peptide self-assembly for nanomedicine, demonstrating favorable properties that mediate drug and gene delivery and ease of preparation.[25, 26] Recently, a dual-domain peptide was developed to incorporate aspects of self-assembly with DNA, cell penetration, endosomal escape, and mitochondrial targeting for gene therapy.[27] Molecular self-assembly to construct nanoscale materials is attractive due to its synthetic simplicity resulting in arrangement of well-defined, ordered architectures.[28] The supramolecular assemblies are dictated by non-covalent interactions such as electrostatic, hydrophobic, van der Waals, and hydrogen bonds amid the backbone and side chain's chemical moieties, driving the formation into steady state positions.[29] A recent study showed that even minor alterations to a peptide sequence along with specific environmental conditions can drastically affect the propensity to self-assemble.[30] Furthermore, specific organic solvents have been shown to affect the self-assembly of polypeptides, DNA, and other polymers, demonstrating a simple method to tune supramolecular structure.[31-33]

In this paper, a facile formulation strategy utilizes solvent-driven forces for self-assembly of an acid-responsive, cationic poly(ketalized serine) [poly(kSer)] peptide and siRNA, resulting in a nanoparticle which efficiently and safely encapsulates siRNA with triggered release upon exposure to mildly acidic conditions.

Materials and methods

Materials

All chemicals purchased from various vendors were used as received without further purification. Anhydrous acetonitrile (CAN), anhydrous tetrahydrofuran (THF), anhydrous ethyl acetate (EtOAc) were purchased from Acros Organics (Thermo Fisher, Pittsburg, PA). Anhydrous dimethylformamide (DMF), dimethylsulfoxide (DMSO), tetrabutylammonium hydroxide (TBAH), ethyl trifluoroacetate, O-tertbutyl-L-serine, branched polyethylenimine (bPEI, 25 kDa) and 3-(4,5-dimethyl-2-thiazolyl)-2,5-diphenyltetrazolium bromide (MTT) were supplied from Sigma Aldrich (St. Louis, MO). Anhydrous dimethylacetamide (DMAc) was purchased from Alfa Aesar (Ward Hill, MA). Ethidium bromide was purchased from Fisher Scientific (Pittsburg, PA). 2-(2-(2-(2-aminoethoxy)ethoxy)ethoxy)ethan-1-ol was purchased from Santa Cruz Biotechnology (Dallas, TX). Silencer anti-GFP siRNA (sense strand 5'-CAAGCUGACCCUGAAGUUCdTdT-3' and antisense strand 5'-GAACUUCAGGGUCAGCUUGdTdT-3'), scrambled siRNA (sense strand 5'-AGUACUGCUUACGAUACGGdTdT-3' and antisense strand 5'-CCGUAUCGUAAGCAGUACUdTdT-3'), and Cy3-labeled control siRNA were purchased from Ambion (Austin, TX). Amicon Ultra Centrifugal filters (MWCO 3 and 30 kDa) were supplied from Millipore (Billerica, MA). Human cervical cancer HeLa cells, mouse lymphoma EL4 cells, ovalbumin (OVA)-expressing mouse lymphoma E.G7-OVA cells were purchased from ATCC (Manassas, VA, USA) and transduced with eGFP-encoding retrovirus and sorted for cells with high eGFP expression using a cell sorter. GFP-expressing HeLa and EL4 cells (HeLa-GFP and EL4-GFP) were cultured in Dulbecco's Modified Eagle Medium (MediaTech, Herndon, VA) supplemented with 10% fetal bovine serum (FBS) (Hyclone, Logan, UT) and 1% antibiotics (100 units/mL penicillin and 100 µg/mL streptomycin, MediaTech). Ovalbumin (OVA)- and GFP-expressing E.G7-OVA cells (E.G7-OVA-GFP) were cultured in RPMI-1640 medium (MediaTech) supplemented with 10% FBS, 50 µM of 2-mercaptoethanol (Invitrogen), 2 mM of L-glutamine (MediaTech), 400 mg L−1 of G418 (MediaTech), 2.5 g L−1 of glucose (MediaTech), 10 mM of HEPES (Media-Tech), and 1 mM of sodium pyruvate (MediaTech). All cells were cultured at 37 °C with 5% CO_2.

Experimental
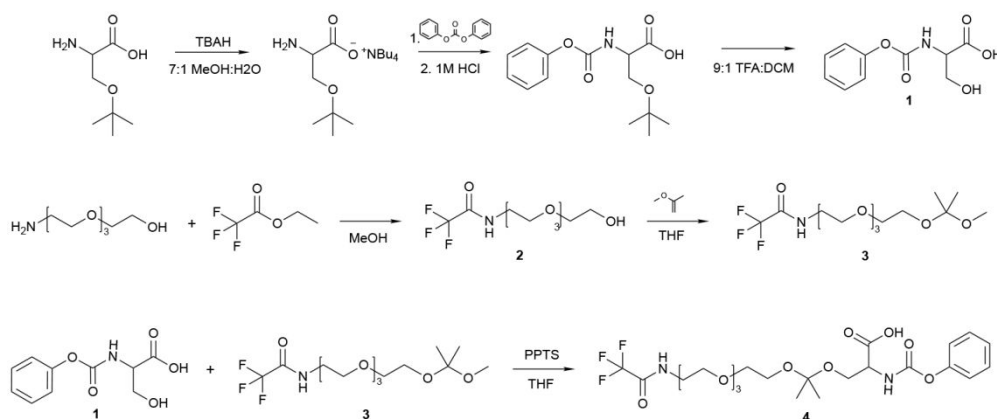
Scheme 1. Synthesis of kSerTFA-urethane monomer.
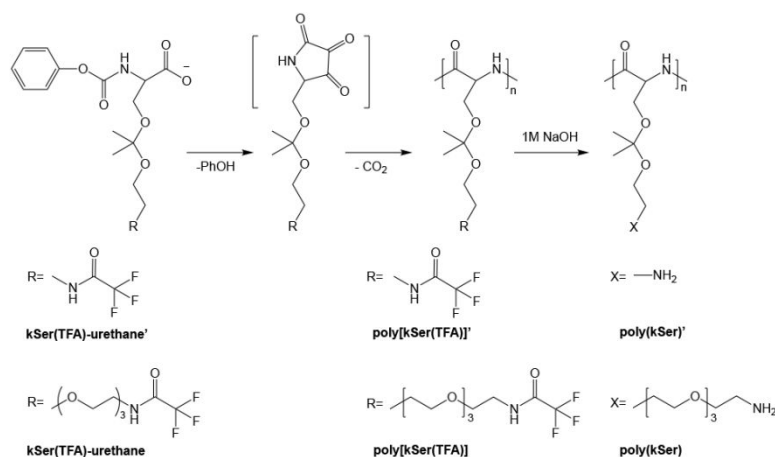
Scheme 2. Polymerization of two different analogues of acid-responsive peptides using urethane derivatives of amino acids. Top: poly(kSer)', bottom: poly(kSer).

Chemical analyses. For all chemical synthesis, ^{1}H NMR spectra were obtained using a Bruker Advance 500 MHz NMR spectrometer (Bruker Biospin Corporation, Billerica, MA). Electrospray mass spectra of intermediates were obtained using a Micromass LCT mass spectrometer (Micromass Ltd., Manchester, UK).

Synthesis of 3-Hydroxy-2-(phenoxycarbonylamino)propionic acid (Compound 1). Compound 1 in **Scheme 1** was synthesized according to the procedures as previously reported.[34]

Synthesis of 2,2,2-trifluoro-N-(2-(2-(2-(2-hydroxyethoxy)ethoxy)ethoxy)ethyl)acetamide (Compound 2). Two grams (10.3 mmol, 1 equiv) of 2-(2-(2-(2-aminoethoxy)ethoxy)ethoxy)ethan-1-ol was added to 10 mL MeOH. 1.57 g (15.5 mmol, 1.5 equiv) trimethylamine was then added. Finally, 1.76 g (12.4 mmol, 1.2 equiv) ethyl 2,2,2-trifluoroacetate was added dropwise and stirred overnight to obtain trifluoroacetamide (TFA)-protected 2-(2-(2-(2-aminoethoxy)ethoxy)ethoxy)ethan-1-ol. Methanol was removed under reduced pressure followed by triple extraction with ethyl acetate in water with a 4:1 ratio. Magnesium sulfate was used to remove residual water in the organic phase, and then the solvent evaporated to recover the final product. The product was recovered as a clear oil (87.2% yield). ^{1}H NMR (500 MHz, DMSO-d_6, δ): 3.36 (q, 2H), 3.43 (t, 2H), 3.52 (m, 12H), 4.58 (t, 1H), 9.49 (s, 1H); (ESI) m/z: [M + Na]$^+$ calcd for $C_{10}H_{18}F_3NO_5$, 312.3; found, 312.2.

Synthesis of N-(3,3-dimethyl-2,4,7,10,13-pentaoxapentadecan-15-yl)-2,2,2-trifluoroacetamide (Compound 3). Compound 2 (2.87 g, 9.9 mmol, 1 equiv) was dissolved in 18 mL dry THF. 0.25 g (0.99 mmol, 0.1 equiv) pyridinium p-toluenesulfonate (PPTS) was then added and stirred for 10 min. 5Å molecular sieves were added to fill a quarter of the solvent and stirred for another 10 min. Lastly, 2.85 mL 2-methoxypropene (29.7 mmol, 3 equiv) was added and stirred for 3 hours on ice. Trimethylamine (TEA) (2 mL) was

added to quench the reaction. The molecular sieves were filtered, and the solvent removed under reduced pressure before purification of final product using silica gel column chromatography using 4:6 hexane:ethyl acetate as eluent. The final product was recovered as a clear oil (62.0% yield). ^{1}HNMR (500 MHz, DMSO-d_6, δ): 1.26 (s, 6H), 3.10 (s, 3H), 3.36 (q, 2H), 3.43 (t, 2H), 3.53 (m, 12H), 9.47 (s, 1H); (ESI) m/z: [M + Na]$^+$ calcd for $C_{14}H_{26}F_3NO_6$, 384.4; found, 384.3.

Synthesis of 1,1,1-trifluoro-16,16-dimethyl-2-oxo-19-((phenoxycarbonyl)amino)-6,9,12,15,17-pentaoxa-3-azaicosan-20-oic acid (kSer(TFA)-urethane, Compound 4). Compound 1 (0.5 g, 2.2 mmol, 1 equiv) was dissolved in 5 mL dry THF followed by the addition of PPTS (0.17 g, 0.66 mmol, 0.3 equiv). After stirring for 10 min, 5 Å molecular sieves were added to the reaction mixture. After another 5 min stirring, Compound 3 (0.96 g, 2.6 mmol, 1.2 equiv) was added dropwise and stirred for 24 h. After sieves were filtered, the product was purified using silica gel column chromatography using 1:3 methanol:ethyl acetate as eluent with addition of 0.3% TEA in the eluent solvent. The product was obtained as oil with hint of yellow color (31.0% yield). ^{1}H NMR (500 MHz, DMSO-d_6, δ): 1.29 (s, 6H), 3.18 (s, 2H), 3.34 (m, 2H), 3.52 (m, 12H), 3.67 (m, 2H), 4.07 (m, 1H), 7.12 (m,3H), 7.22 (t, 1H), 7.39 (t, 2H), 7.54 (m, 1H), 9.53 (s, 1H); (ESI) m/z: [M + Na]$^+$ calcd for $C_{23}H_{33}F_3N_2O_{10}$, 577.5; found, 577.3.

Synthesis and characterization of acid-transforming polypeptide. Acid-responsive polypeptides were synthesized using previously reported procedures (**Scheme 2**).[34] Briefly, the monomers were added to an oven-dried glass vial and the air was removed via high vacuum for 10 min. Subsequently, anhydrous acetonitrile was added to a final concentration of 0.28 M. The reaction was stirred at room temperature overnight and solvent was removed using high vacuum. The molecular weight of polypeptide was determined by MALDI/TOF (AB Sciex TOF/TOF 5800, Foster City, CA). All polymerized polypeptides were first deprotected of TFA group in 1 M NaOH overnight to

obtain final peptide before molecular weight measurement using 2,5-dihydroxybenzoic acid as the matrix material for molecular weight analysis. The samples were irradiated with 349 nm diode-pumped solid state Nd:YAG laser and detected on linear high mass positive mode. M_w, M_n, polydispersity index (PDI) (M_w/M_n) was determined using Data Explorer software where the Polymer Analysis Toolbox function was used on the gated range of the molecular weight peaks. The degree of polymerization (DP) was determined approximated based on the molecular weight of the individual amino acid residue.

Self-assembly of acid-responsive peptides

Urethane monomers were added to an oven-dried glass vial and the air was removed via high vacuum for 10 min. Subsequently, anhydrous solvent (ACN, DMF, THF, DMAc, DMSO, EtoAc) was added to a final concentration of 0.28 M. The reaction was stirred at room temperature overnight. After polymerization, acetonitrile was removed using high vacuum and TFA-protected peptides were re-suspended in the same volume of water. In order to investigate the effects of amino terminus on self-assembly in acetonitrile, amino terminus on peptide was exposed using 1 M NaOH overnight for deprotection of TFA. Subsequently, the peptide was purified using centrifugal filtration with molecular weight cutoff 3,000 Da, spinning at

3,800 rpm at 4 °C for 4 washes. Peptides were re-suspended in acetonitrile to a concentration of 0.28 M. A 2 µL aliquot of the peptide/siRNA complexes in 80% (v/v) acetonitrile/water was deposited onto a carbon-coated copper TEM (Ted Pella, Redding, CA), and allowed to completely dry in air followed by additional drying in a vacuumed chamber for 20 min. Uranyl acetate staining (1% in water) was applied onto the grid and allowed to air dry for 24 h before viewing under transmission electron microscope at 200 kV (Phillips electronic Instruments, Mahwah, NJ). For samples dispersed in water, 8 µL of the sample was deposited onto the surface of the grid for 10 min before water removal and uranyl acetate staining and left to air dry overnight. Different anhydrous solvents (DMF, THF, DMAc, DMSO, EtoAc) were used in place of acetonitrile while following the same procedure used for polymerization.

Preparation of poly(kSer)/siRNA complexes in acetonitrile/water mixture. 1 µg siRNA in 10 µL DI water was added dropwise to a total volume of 23 µL peptide dissolved in DI water and vortexed briefly before incubating for 15 min at room temperature (different N/P ratios were achieved by varying amounts). Acetonitrile (128 µL) was added directly to the peptide/siRNA mixture to achieve 80% (v/v) acetonitrile/water and incubated for another 10 min. A 2 µL
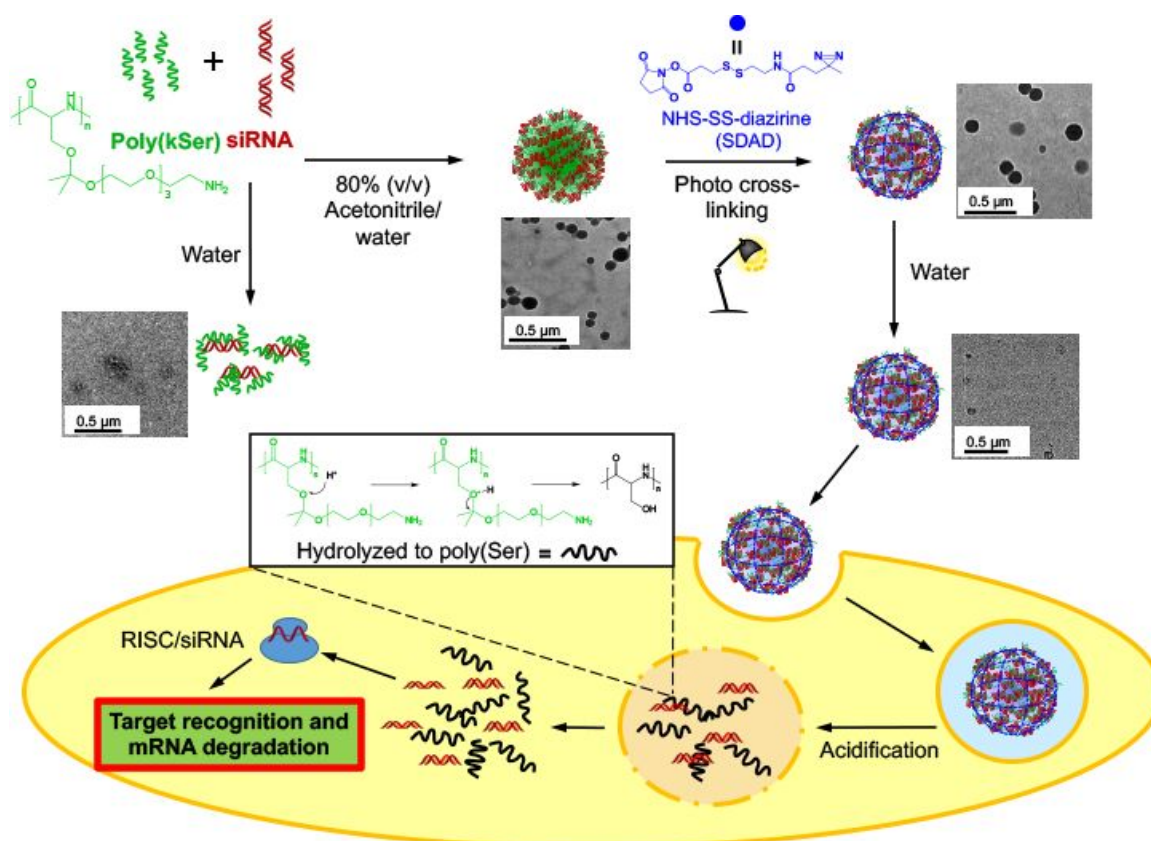

Figure 1. *Schematic illustration of poly(kSer)/siRNA nanoparticles using solvent-driven self-assembly with respective TEM images. Poly(kSer)/siRNA prepared in water at N/P ratio of 20 results in no detectable nanoparticles. Acetonitrile added to a final 80% (v/v) acetonitrile/water concentration results in uniform, stable nanoparticles. NHS-SS-diazirine is used to photo cross-link for further stabilization in water. After cellular uptake, acid-triggered hydrolysis of poly(kSer) to poly(Ser) assists in endosomal escape, disassembly, and intracellular trafficking for RNAi.*

aliquot of the peptide/siRNA complexes was used for TEM as described earlier.

Synthesis of cross-linked poly(kSer)/siRNA Complexes. Acid-responsive, cross-linked poly(kSer)/siRNA complexes were synthesized as illustrated in **Figure 1**. Poly(kSer)/siRNA complexes were prepared in DI water at N/P ratio of 20, where 1 µg siRNA in 10 µL DI water was added dropwise to peptide in a total volume of 23 µL and incubated for 15 min. Different mole % of amines (e.g., 10 or 50) on peptide was reacted with succinimidyl 2-[(4,4′-azipentanamido)ethyl]-1,3′-dithioproprinate (NHS-SS-Diazirine or SDAD) (Thermo Scientific, Rockford, IL) dissolved in DMSO for 2 h at 4°C. Excess unconjugated SDAD was removed using centrifugal filtration with molecular weight cutoff of 30 kDa, spinning at 13,200 RPM for 5 min, and washing twice with DI water. The concentrated diazirine-functionalized peptide/siRNA complexes were recovered and 128 µL acetonitrile was added to achieve 80% (v/v) acetonitrile/water and incubated at room temperature for 10 min. Then, 365 nm wavelength UV light was irradiated directly onto the sample for 30 min to initiate cross-linking with the unreacted amines or any nucleophiles on the surface. Then, acetonitrile was removed via high vacuum, and the stabilized particles were re-dispersed in 500 µL water.

DNA condensation, size, and surface charge of cross-linked and non-cross-linked poly(kSer)/siRNA complexes. The siRNA condensation efficiency was determined using the ethidium bromide (EtBr) exclusion assay. Briefly, cross-linked poly(kSer)/siRNA complexes were prepared using the methods as previously outlined but with siRNA (1 µg) mixed with 0.25 µg EtBr before stabilization. Controls include non-cross-linked poly(kSer)/siRNA complexes and 25 kDa bPEI/siRNA complexes at N/P 10. Fluorescence intensity of unshielded siRNA was measured using a fluorescence plate reader (BioTek Synergy H1, Winooski, VT) at excitation and emission wavelength of 320 and 600 nm, respectively. The fluorescence was normalized to that of free siRNA. The average diameter and zeta-potential of cross-linked poly(kSer)/siRNA complexes were measured using dynamic light scattering using a Zetasizer Nano-Zs (Malvern, Instruments Ltd., Worcestershire, UK). Non-cross-linked peptide/siRNA complexes were prepared by adding siRNA and poly(kSer) in DI water dropwise, vortexed, and incubated at room temperature for 15 min. To evaluate complexation, EtBr exclusion assay was performed as described earlier.

Acid hydrolysis of cross-linked poly(kSer)/siRNA and kinetics of siRNA release. Cross-linked and non-cross-linked poly(kSer)/siRNA complexes were subjected to agarose gel electrophoresis after incubation under acidic conditions to test for acid-responsive siRNA release. Acetate buffer (100 mM, pH 5.0) was added to the peptide/siRNA complexes at 1:1 volume and incubated at 37°C for 4 h. After 4 h hydrolysis, the volume was concentrated using centrifugal filtration at 3,000 Da molecular weight cut off and spinning at 13,200 rpm for 5 min. The retained sample was collected and ran on a 1% agarose gel to observe siRNA release before and after acid-hydrolysis. siRNA

was also quantified before and after acid hydrolysis using RNA quantification kit (Quant-iT RNA Assay Kit, Life Technologies). The kinetics of acid release was also investigated. Cross-linked poly(kSer)/siRNA complexes carrying 1 µg siRNA were prepared with the same procedures mentioned above. 1:1 volume of 100 mM acetate buffer at pH 5.0 or 1X PBS at pH 7.4 was added and incubated at 37°C. At various time points of 0, 0.5, 1, 2, 4, 8, 12, and 24 h, siRNA release was investigated using 1% agarose gel electrophoresis. Released siRNA was also quantified using RNA quantification kit.

In vitro gene silencing and cytotoxicity of cross-linked poly(kSer)/siRNA complexes. HeLa-GFP cells were plated in DMEM containing 10% FBS at a density of 50,000 cells/well in a 24-well plate 24 h prior to transfection. The cross-linked poly(kser)/siRNA complexes were first prepared for a dose-dependent gene silencing study using anti-GFP siRNA and siRNA with a scrambled sequence (Scr siRNA). The final volume of the cross-linked poly(kSer)/siRNA complexes was concentrated down to 35 µL using centrifugal filters with molecular weight cutoff of 30 kDa. The complexes were supplemented with 1X PBS prior to adding directly to cells in 0.3 mL serum-free media for 4 h. The different doses of siRNA delivered in 0.3 mL serum-free media were 0.27, 0.54, 1.1, or 2.2 µM corresponding to 1, 2, 4, or 8 µg siRNA/well respectively. After 4 h of incubation, the medium was replaced with fresh DMEM containing 10% FBS, and the cells were further incubated for 3 days before assessing GFP silencing using Guava EasyCyte Plus flow cytometer (Guava Technologies, Inc., Hayward, CA). 25 kDa bPEI at N/P ratio of 10 carrying 1 µg siRNA was used as the control. Specific gene silencing was assessed by normalizing against cells treated with its respective dose of Scr-siRNA. E.G7-OVA-GFP cells later used for gene silencing *in vivo* were also used to assess gene silencing and were plated at 50,000 cells/well on the day of transfection following similar transfection protocols.

Cytotoxicity of cross-linked poly(kSer)/siRNA complexes at various doses (0.27 µM, 0.54 µM, 1.1 µM, or 2.2 µM) was quantified using the conventional MTT assay. Cross-linked poly(kSer)/siRNA complexes were prepared using 0.2 µg siRNA for the lowest siRNA amount to 10,000 HeLa-GFP cells/well plated in a 96-well plate 24 h prior to transfection. The cross-linked poly(kSer)/siRNA complexes in water was supplemented with 1X PBS before adding directly to cells in 60 µL serum-free media. After the 4 h of incubation, the medium was replaced with 200 µL fresh DMEM media containing 10% FBS for another 24 h before conducting MTT assay. MTT in PBS (0.5 mg/mL) was added to cells in a final volume of 100 µL complete media for 2 h. Subsequently, the medium was removed and 200 µL DMSO was added to dissolve the formazan crystals. The relative viability of the cells was assessed by measuring UV absorbance at 561 nm.

Cellular uptake of cross-linked poly(kSer)/siRNA. The cellular uptake of poly(kSer)/siRNA complexes was investigated using confocal laser scanning microscopy. Cy3-labled siRNA at 1 µg or 4 µg was used for preparation of cross-linked poly(kSer)/siRNA complexes using the method described above. 30,000 HeLa-GFP

cells were plated on a 8-well culture slide 24 h prior to transfection. Cells were transfected with same procedures outlined above. After 4 h of incubation, the media was removed and the nuclei of cells were stained with NucBlue Live Cell Stain (Molecular Probes, Life Technologies, OR) for 5 min, washed twice with PBS, fixed with 4% *p*-formaldehyde for 10 min, and further washed twice with PBS, all done under dark conditions. Cells were analyzed using Olympus IX2 inverted microscope equipped with a Fluoview 1000 confocal laser scanning microscopy setup (FV10-ASW, Olympus America, Melville, NY). The cells were scanned in three dimensions using z-stacking, and an image traversing the middle of the cellular height was used for analysis.

In vivo GFP silencing. C57BL/6 mice (8 week-old female) were purchased from Charles River Laboratories (Wilmington, MA) with the approval of the Institutional Animal Care and Use Committee (IACUC) at University of California, Irvine. Mice were kept under anesthesia using isoflurane inhalation during the procedures to minimize pain and discomfort. Tumors were first established using subcutaneous injection of 1×10^6 E.G7-OVA-GFP cells at the flank and monitored for 1 week before

administrating poly(kSer)/siRNA complexes through tail vein injection. Poly(kSer)/siRNA complexes were prepared using 20 µg anti-GFP siRNA with the same procedures as outlined before. After three days post injection, tumors were harvested and IVIS Lumina (Caliper Life Sciences, Hopkinton, MA) was used to measure epi-fluorescence.

Statistical analysis. All data collected represented as mean ± standard deviation. Statistical analysis was performed with Student's *t* Test with statistical significance at *p*-values lower than 0.05.

Results and Discussion

Solvent-driven self-assembly of acid-responsive polypeptides

Several factors control the self-assembly of peptides, including pH, amino acid composition, and solvent effects.[35, 36] Organic solvents have been previously used to induce peptide self-assembly, and it was recently shown that even minute amounts of solvent can influence non-covalent interactions to change self-assembly arrangements.[37-39] Since poly(kSer) is acid-
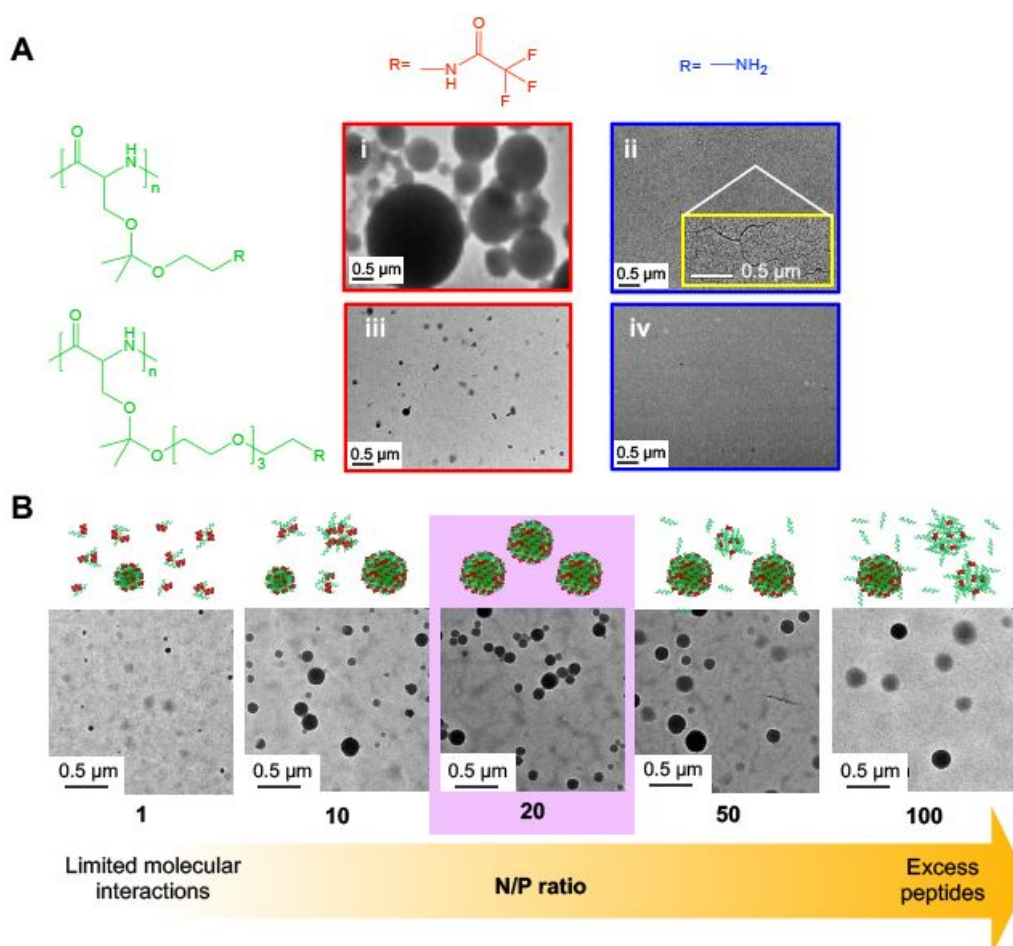

Figure 2. *A. TEM images of acid-responsive peptides with trifluoroacetamide (TFA) end group in acetonitrile (i and iii) and amino termini in water (ii and iv). B. Schematic illustration and TEM images of poly(kSer)/siRNA complexes in 80% (v/v) acetonitrile/water at different N/P ratios.*

sensitive and comprised of a repeating amino acid derivative, we chose to focus on solvent effects for its self-assembly. **Figure 2A** depicts four variations of the acid-responsive poly(ketalized serine) used in this study: poly(kSer) and poly(kSerTFA) both bear an extended oligo(ethylene oxide) moiety on each serine side chain to improve solubility (TFA denotes the trifluoroacetamide group on each serine side chain); poly(kSer)' and poly(kSerTFA)' have a shorter, more hydrophobic chain per each serine residue. Although the TFA-protected peptides lack the multiple amines capable of siRNA complexation, they were selected to understand the self-assembly mechanism. The peptides were synthesized according to the previously reported polymerization method utilizing urethane-functionalized monomers (**Scheme 2**).[34] Molecular weight analysis using MALDI-TOF revealed high molecular weight peptides of approximately 127 residues for poly(kSer)' and 84 residues for poly(kSer) with low polydispersity index (PDI) of 1.15 and 1.18, respectively (**Table S1**).

Transmission electron microscopy (TEM) was taken at various steps throughout the synthesis of the peptides in acetonitrile, where both poly(kSerTFA) and poly(kSerTFA)' self-assembled into spherical nano- and microparticles, respectively (**Figure 2A-i and 2A-iii**). Poly(kSerTFA)' formed larger, heterogeneous, particles whereas poly(kSerTFA), having more hydrophilic side chains, exhibited smaller homogeneous architectures. To further evaluate the solvent forces directing these assemblies, the peptides were transferred into water and examined under TEM. Both peptides saw a reduction in the amount of self-assembled particles: poly(kSerTFA)' maintained a few spherical assemblies with reduced diameter, whereas poly(kSerTFA) indicated no retention of structured particles, likely due to the additional oligo(ethylene oxide) chains increasing solubility (**Figure S1**). This indicates that the molecular properties of acetonitrile largely contributed to the molecular assembly of the polypeptides. Different solvents were tested in the polymerization to understand how polarity of solvent may affect the self-assembly process (**Figure S2**). Since acetonitrile is a polar aprotic solvent, it was anticipated that other polar aprotic solvents like dimethylformamide (DMF), tetrahydrofuran (THF), dimethylacetamide (DMAc), dimethylsulfoxide (DMSO), and ethyl acetate (EtoAc) would also induce the effect. Poly(kSerTFA)' was chosen for this since it featured larger and more prominent self-assembly than its counterpart. The tested solvents failed to produce self-assembled particles comparable to those observed using acetonitrile, only minor aggregation and association was observed. A recent investigation into the structural dynamics of a monomeric polyglutamine peptide revealed that hydrogen bonding amongst side chain amide groups was a major factor in formation of β-sheet structures in acetonitrile.[40] Although it is speculated that the side chain amide groups of poly(kSerTFA) and poly(kSerTFA)' contribute to self-assembly in acetonitrile via intramolecular hydrogen bonding, further studies are needed to determine the exact mechanism by which this occurs.

To gain further insight into peptide structure and its assembly, poly(kSer) and poly(kSer)' were tested in acetonitrile

and water. Even with the TFA groups removed, poly(kSer)' had very limited solubility in water, as shown by the formation of threadlike structures (**Figure 2A-ii**). The low solubility results from the hydrophobic ketal branches and aliphatic chains on a high molecular weight peptide. Its analogue, poly(kSer), however, consisting of multiple ethylene oxide groups, was completely soluble (**Figure 2A-iv**). As poly(kSer) was placed back into acetonitrile, limited assemblies formed (**Figure S1-iii**), indicating that self-assembly in acetonitrile is inhibited by the peptide's multiple primary amines and its consequent increased polarity. Further studies may be done incorporating a wide range of terminal moieties with various polarities and chemical properties, including secondary and tertiary amines, to investigate how these properties affect self-assembly in addition to molecular dynamics studies. Furthermore, these acid-responsive peptides may be explored for targeted delivery of small-molecule therapeutics.

Self-assembled, cross-linked acid-responsive polypeptides with siRNA complexation

siRNA is not completely soluble in acetonitrile, and a complex of poly(kSer)/siRNA in acetonitrile was hypothesized to be entropically favored[41, 42] for self-assembly, therefore poly(kSer)/siRNA complexes were first prepared in minimal amounts of water. Poly(kSer) and siRNA were mixed at various N/P ratios in minimal amounts of water to first form electrostatic interactions. It should be noted that poly(kSer)' was found to not complex siRNA very effectively in water, most likely due to low cationic density as well as steric hindrance from bulky methyl ketal moieties (**Figure S3**). Figure 1 TEM image indicated very faint yet loosely aggregated poly(kSer)/siRNA in water, with the majority of TEM area blank. Furthermore, other quantification methods were used such as dynamic light scattering and zeta potential to assess particle formation/parameters, yet no particles were detected. When poly(kSer)/siRNA complexes were added with acetonitrile to make 80% (v/v) acetonitrile/water mixture, well-defined spherical nano-sized particles were observed (**Figure 2B**). The process of self-assembly depends on a fine-tuned balance between intramolecular interactions within the peptide structure and peptide-solvent interactions.[43] Additional hydrophobic interactions and internal pressure effects further contribute to structural stabilization during self-assembly.[44] Water-acetonitrile mixtures have a partially hydrophobic character, therefore poly(kSer)' having more hydrophobic side chains would have disrupted tertiary structures.[41] Poly(kSer), having more hydrophilic character behaved similarly in more polar solvent, in this case water, due to greater peptide-solvent interactions than intramolecular hydrogen bonding. The addition or removal of the trifluoroacetamide group presents another facet of self-assembly, where the free amines can induce cation-dipole interactions with amide carbonyls, completely changing tertiary structures.[43] The self-assembly of poly(kSer)siRNA complexes in 80% acetonitrile indicate that the ionic interaction between poly(kSer) side chain amines and siRNA phosphate backbone favourably contributes to the interplay of peptide-solvent interactions. As the N/P ratio

increased from 1 to 20, the number and size of particles increased. Starting from N/P ratio of 50 to 100, the formation of a mixture of obscurely faint and dense particles was observed on TEM. It is speculated that at N/P ratios of 50 to 100, excess peptide was present causing the formation of faint particles, which may be consisting of partial interaction with siRNA or peptide itself. Therefore, N/P ratio of 20 was chosen for further studies.

For safe in vitro and in vivo administration of the self-assembled poly(kSer)/siRNA particles, all traces of acetonitrile must be removed and must remain intact while in aqueous buffer. Using only the solvent-driven assembly process in acetonitrile, the transfer of particles back into water completely disrupted the interaction between poly(kSer) and siRNA (data not shown). Therefore, the poly(kSer)/siRNA complexes were stabilized using a photo-initiated crosslinker. Briefly, succinimidyl 2-[(4,4′-azipentanamido)ethyl]-1,3′-dithioproprionate (NHS-SS-Diazirine or SDAD) was used to cross-link the amine groups available on the surface of poly(kSer)/siRNA complexes in acetonitrile (**Figure 1**). The SDAD crosslinker disulfide bond can be reduced to enhance the breakdown and biocompatibility of the poly(kSer)/siRNA complex, while incorporating an additional layer of control over release kinetics with a slower breakdown of the disulfide bond.[45] Cross-linked poly(kSer/siRNA) maintained well-defined

spherical structure when placed in 80% (v/v) acetonitrile/water. Either 10 or 50 mole % of amines on the peptide was used for diazirine-functionalization using NHS chemistry (**Table S2**). Conjugation with 50 mole % of amines resulted in stabilized particles of approximately 150 nm in diameter with low PDI of 0.225 after removal of solvent and re-dispersing into water. Conjugation with 10 mole % of amines resulted in incomplete cross-linking having large particle sizes greater than 300 nm and PDI greater than 0.5, indicating incomplete stabilization (**Table S2**). The zeta potential of cross-linked poly(kSer)/siRNA was slightly negative (-1.2 mV), signifying that a majority of exposed amines were utilized for cross-linking (**Table S2**). This also indicates that surface charges of poly(kSer)/siRNA can be tailored by the degree of cross-linking. The low anionic surface charge of the cross-linked poly(kSer)/siRNA may reduce adverse interactions with serum proteins, suggesting suitability for in vivo applications. Furthermore, tunability of surface further allows for additional modifications to enable targeted delivery or conjugation of other agents for combination therapies.

Acid-responsive siRNA release from cross-linked poly(kSer)/siRNA complexes

SDAD cross-linked poly(kSer)/siRNA complexes demonstrated retention of siRNA using gel electrophoresis, and the conventional ethidium bromide (EtBr) exclusion assay revealed
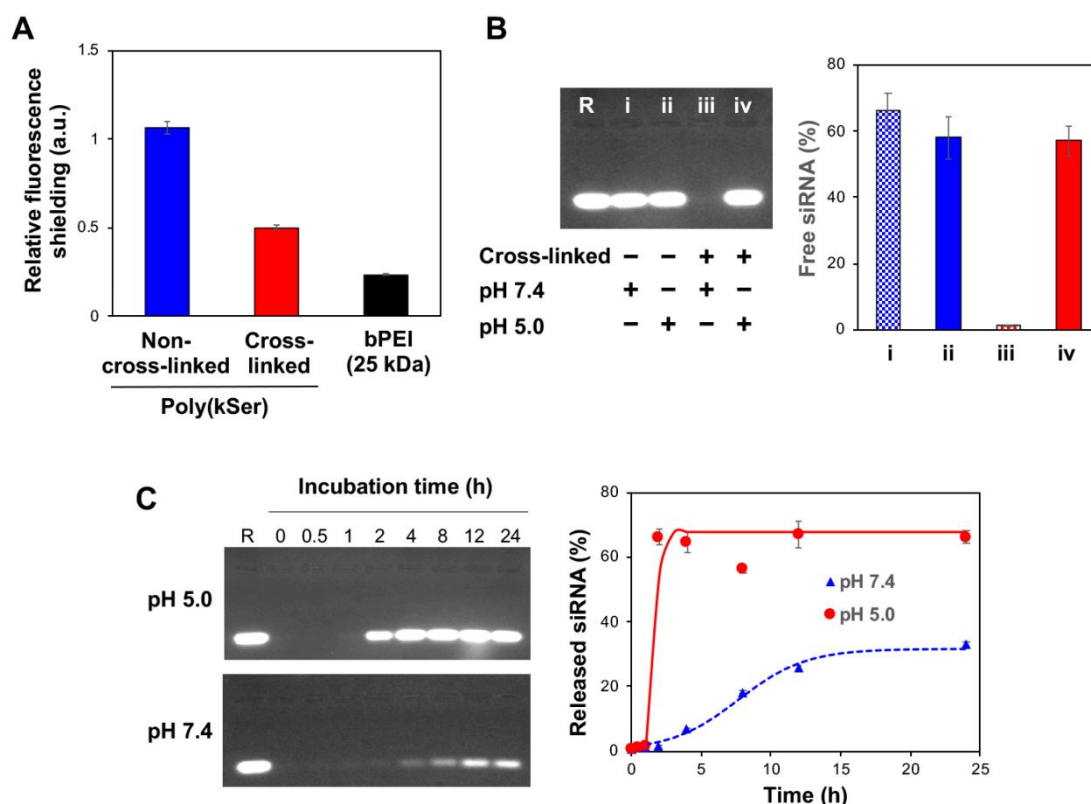

Figure 3. *A. Ethidium bromide exclusion assay showing fluorescence shielding of non-cross-linked and cross-linked poly(kSer)/siRNA complexes. B. Agarose gel electrophoresis and RNA quantification of non-cross-linked and cross-linked poly(kSer)/siRNA complexes at neutral (pH 7.4) and acidic (pH 5.0) conditions. C. Agarose gel electrophoresis and RNA quantification showing kinetics of siRNA release in acidic (pH 5.0, top) and neutral (pH 7.4, bottom) conditions at 37°C. R in agarose gel electrophoresis represents 1 μg free siRNA as the control.*

a reduction in fluorescence shielding in contrast to the non-cross-linked complexes. However, cross-linked poly(kSer)/siRNA exhibited higher EtBr fluorescence than 25 kDa bPEI (**Figure 3A**), indicating that some siRNA may be partially exposed on its surface as the negative zeta potential indicates.   RNA quantification showed that non-cross-linked complexes had approximately 66.2% free siRNA whereas stabilized, cross-linked complexes showed a vast reduction to 1.15% free siRNA (**Figure 3B**). Additionally, the acid-responsive property of poly(kSer) was demonstrated by incubating the complexes at pH 5.0 acetate buffer for 4 h and assessing siRNA release. Acid-hydrolysis of poly-ketalized serine was previously confirmed using NMR.[22] **Figure 3B** shows approximately 57% of the encapsulated siRNA was released under slightly acidic conditions, compared to a negligible amount released at pH 7.4. The cross-linked complexes clearly demonstrate the capability to encapsulate siRNA while releasing under specific conditions. These self-assembled complexes represent an efficient and facile method to utilize RNAi therapy while ensuring release upon exposure to the environment of the endosome, an important aspect for siRNA delivery.[46]

siRNA release kinetics from the carrier is a major factor defining the effectiveness of RNAi therapy,[47] so the kinetics of siRNA release from the acid-responsive peptide was compared at different pHs (5.0 and 7.4) at 37°C to mimic intracellular conditions (**Figure 3C**). The gel electrophoresis images and RNA quantification both indicate greater quantity of siRNA released in shorter time frames under acidic conditions compared to neutral pH. Within the first hour, minimal siRNA was detected in the acidic condition, but after 2 h, a substantial amount of hydrolysis caused a drastic increase in siRNA release. At 4 hours, nearly 70% of siRNA was released, and a plateau was reached. Conversely, when treated with pH 7.4 PBS buffer, a negligible amount of siRNA was detected for the first 4 hours, finally releasing only 32.9% after 15 h of incubation. The rate of siRNA release remained low at pH 7.4 demonstrating stability of the complexes under physiological conditions, whereas release was abrupt when treated with mildly acidic buffer, exemplifying fast release under acidic cues such as the endosomal environment. Release under these conditions allows for high specificity and stability while in circulation, desirable qualities for an RNAi therapeutic to avoid premature degradation and rapid delivery to the cytoplasm.

Cytotoxicity and gene silencing efficacy of cross-linked poly(kSer)/siRNA complexes

A dose-dependent study was performed to assess cytotoxicity of cross-linked poly(kSer)/siRNA complexes (**Figure 4a**). Tolerable toxicity levels, such as cell viability higher than 80%, was obtained for doses of 0.27, 0.54, and 1.1 μM siRNA, corresponding to 1, 2, and 4 μg siRNA per well, respectively. At 2.2 μM or 8 μg siRNA per well, cell viability decreased to around 63%. The complexes showed low toxicity up to a high dosage of 4 μg siRNA per well. Polyplexes of 25 kDa bPEI and siRNA, administering only 1 μg siRNA, resulted in 63% viability, demonstrating the significantly lowered toxicity of the

poly(kSer)/siRNA complexes. The low toxicity of poly(kSer)/siRNA complexes is attributed to the slightly anionic surface charge and its transformation to a natural, neutral, and biodegradable polyserine upon acid hydrolysis. This further establishes high versatility and potential clinical application of cross-linked poly(kSer)/siRNA complexes as a safe alternative to bPEI, known to be toxic to cells.

Subsequently, the dose-dependent gene silencing study was conducted on HeLa-GFP cells. Gene silencing of approximately 32% at a dose of 4 μg siRNA/well was achieved (**Figure 4B-D**). At lower siRNA doses, such as 1 or 2 μg siRNA/well, gene silencing was negligible and further studies were later conducted to understand the rationale behind this. The highest gene knockdown obtained by cross-linked poly(kSer)/siRNA at 4 μg siRNA/well compares similarly with 25 kDa bPEI at N/P ratio of 10, but unlike high molecular weight bPEI vectors, poly(kSer)/siRNA displays low cytotoxicity and efficient siRNA release. EG7-OVA-GFP suspension cells were also tested for gene silencing in exploration of a gene silencing study *in vivo*. Cross-linked poly(kSer)/siRNA displayed approximately 31% silencing and compares similarly with 25 kDa bPEI, which showed 30% gene knockdown (**Figure S4**). Although higher than typical dosages were required, the efficacy matched closely to the gold standard of 25 kDa bPEI. The cytotoxic nature of high molecular weight bPEI vectors precludes their use for RNAi therapy, thus these cross-linked poly(kSer)/siRNA particles represent a safe, efficient alternative.

To understand why a moderately high dosage of siRNA was needed to show gene silencing effects, confocal laser scanning microscopy was used to visualize cellular uptake, using Cy3-labled siRNA. Confocal microscopy images revealed that while 25 kDa bPEI/siRNA polyplexes had very localized punctate red signal at 4 h of incubation, 1 μg- and 4 μg-treated cells using cross-linked poly(kSer)/siRNA complexes showed siRNA dispersed in the cytoplasm (**Figure 4D** and **Figure S5**). Delivering 4 μg siRNA showed a higher density of siRNA in the cytoplasm than 1 μg. Overall, this demonstrates that cross-linked poly(kSer)/siRNA complexes are taken up by the cells despite the slight anionic surface charge. siRNA being dispersed in the cytoplasm using cross-linked poly(kSer)/siRNA complexes may indicate enhanced rapid endosomal escape properties compared with 25 kDa bPEI/siRNA polyplexes. Hydrolysis of ketal branches possibly increased osmotic pressure and prompted rupture of the endosome.[48] Gene silencing is dependent on many factors including endosomal escape, de-complexation from carrier, and stability in cytoplasm.[49] While the results from confocal imaging indicate efficient endosomal release of poly(kSer)/siRNA compared to bPEI/siRNA, the aforementioned processes must collectively work to increase gene silencing. If the crosslinking negatively affected the de-complexation of siRNA from poly(kSer), this could counteract the benefit from enhanced endosomal escape. Furthermore, the slow breakdown of the disulfide bond from the crosslinker may further contribute to the poly(kSer)/siRNA prolonged complexation within the cytoplasm.[45] This incomplete disassembly of the complexes is hypothesized to cause the high dosage requirement of siRNA to achieve efficient gene
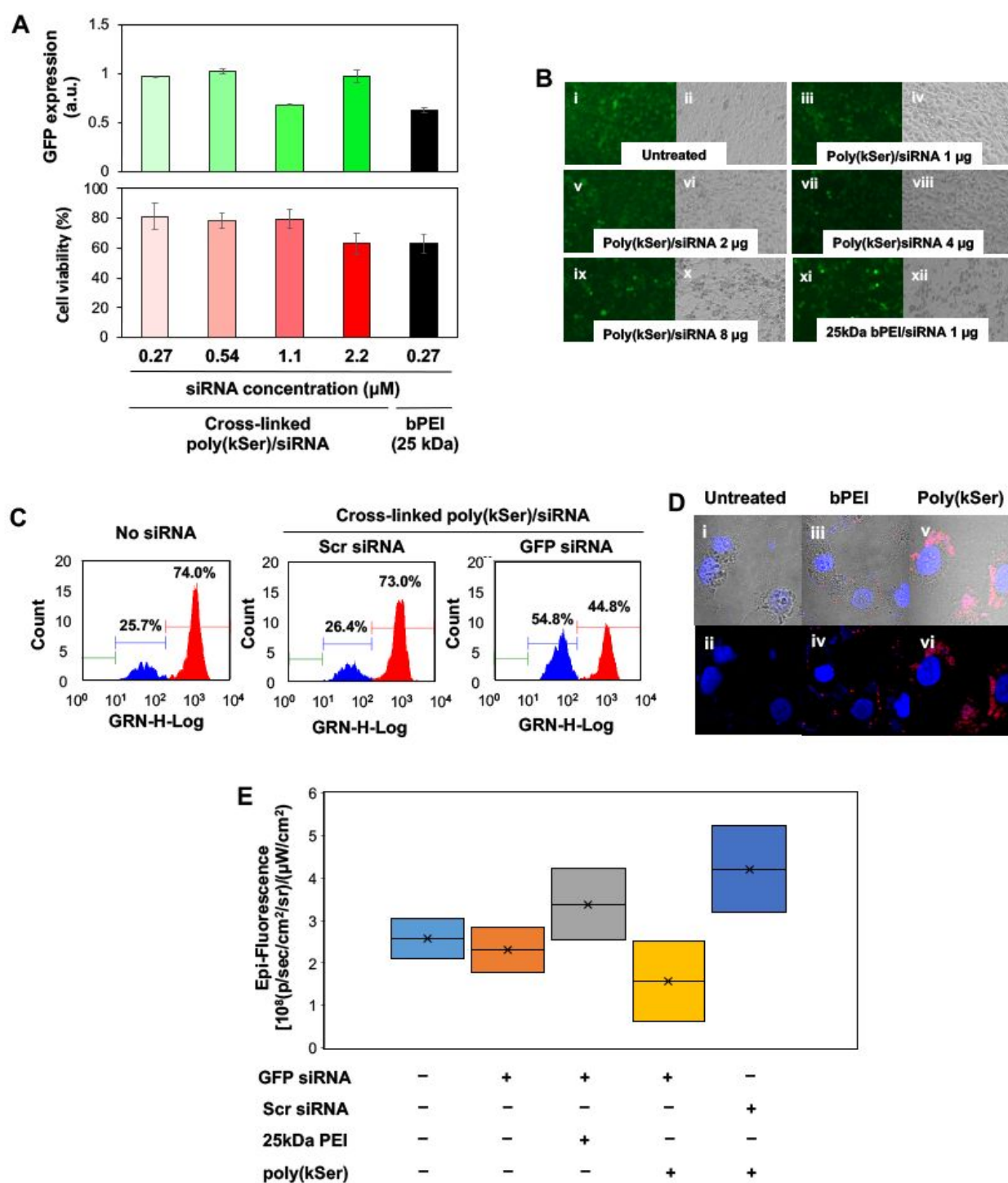
Figure 4. *A. Dose-dependent specific gene silencing of cross-linked poly(kSer)/siRNA measured by flow cytometry and dose-dependent cell viability of cross-linked poly(kSer)/siRNA using MTT assay. B. Fluorescence and bright field microscopy images of i-ii.) HeLa-GFP cells, iii-iv.) cross-linked polyk(Ser) delivering 1 μg siRNA, v-vi.) 2 μg siRNA, vii-viii.) 4 μg siRNA, ix-x.) 8 μg siRNA, xi-xii.) 25 kDa bPEI delivering 1 μg siRNA. C. Flow cytometry histograms demonstrating eGFP gene silencing. D.) Confocal laser scanning microscopy of i-ii.) HeLa-GFP cells, iii-iv.) cells treated with 25 kDa bPEI/siRNA delivering 1 μg Cy3-labeled siRNA, v-vi.) cells treated with cross-linked poly(kSer)/siRNA delivering 4 μg Cy3-labeled siRNA at 4 h. E. Epi-fluorescence quantification of harvested tumors after mice were treated with cross-linked poly(kSer)/siRNA complexes and controls.*

silencing. Since the cross-linking stabilization occurs after complexation between poly(kSer) and siRNA in the synthetic method, there remains a possibility that the free amines of siRNA bases can be covalently cross-linked. This may be

explored through the use of alternative cross-linkers, and as previously discussed, by alternative moieties on the peptide itself. Since the cross-linking feature was included to ensure poly(kSer)/siRNA complexation remained in aqueous buffer for gene knockdown evaluation, future work will focus on modifications to the chemical makeup to ensure self-assembly and stability without crosslinking. Furthermore, these studies can include the use of FRET (Förster resonance energy transfer) to further elucidate any remaining interactions between siRNA and peptide, along with other chemical modifications to ensure complete hydrolysis and disassociation of siRNA.

Due to the particles having sufficient siRNA complexation efficiency, cellular uptake, endosomal escape properties, moderate silencing, and low toxicity in vitro, a preliminary study was performed to assess in vivo toxicity and siRNA delivery. C57BL/6 mice were subcutaneously injected with E.G7-OVA-GFP cells on their flank to establish a tumor. After tumors were established, the mice were injected with cross-linked poly(kSer)/siRNA complexes and other controls (saline, free siRNA, 25 kDa bPEI/siRNA polyplexes, and cross-linked poly(kSer)/Scr siRNA complexes) via tail vein injection and left alone for 3 days until tumors were harvested and the epi-fluorescence (measured by the radiant efficiency) was determined on all tumors. Mice treated with cross-linked poly(kSer)/siRNA complexes displayed a moderate decrease in fluorescence, demonstrating potential in vivo gene knockdown (**Figure 4E**). Anomalous results were observed with both the poly(kSer)/Scr and PEI/siRNA complexes with slightly increased fluorescence though not statistically significant, but it is important to note some limitations of using GFP reporting imposed by tumor microenvironment and heterogeneity. [50] Differing levels of GFP expression prior to treatment may further account for the unexpected results, and future work aims to address these issues by expanding the in vivo study with optimally formulated nanoparticles. Additionally, exploring other targets such as pro-cancer genes for the E.G7-OVA model and/or utilizing other disease models will be used in future work to evaluate the nanoparticles in vivo. Importantly, no in vivo toxicity was observed after administration of poly(kSer)/siRNA complexes, signifying their safety and potential for clinical use. This serves as a basis to proceed with future research on optimizing chemical attributes of the poly(kSer)/siRNA complexes and subsequent expanded in vivo testing.

Conclusions

In this study, we developed a new formulation strategy for constructing effective siRNA carriers from acid-responsive poly(kSer) through self-assembly and photo-crosslinking in acetonitrile. The method offers simplicity in formulation and ease in creating well-defined homogenous carriers, essential properties for consistent clinical efficacy, cost, and scalability. The self-assembled, photo-crosslinked poly(kSer)/siRNA complexes demonstrated efficient siRNA encapsulation and subsequent rapid release r under slightly acidic conditions, prompting fast accessibility and usage in cells. High cell viability was preserved due to low anionic surface charge and high

biocompatibility after hydrolysis-induced transformation into poly(Ser). Higher dosages of siRNA were required, possibly due to incomplete disassembly of poly(kSer)/siRNA complexes, and future work can explore these associations through the use of FRET and molecular dynamics studies and exploration of alternative crosslinkers. Further studies to optimize poly(kSer)/siRNA complexes may include varying chemical moieties of each kSer residue to enhance self-assembly, hydrolysis, and siRNA disassociation upon environmental cues. Alternative chemical modifications may open possibilities for other organic solvents to drive self-assembly, eliminate the need for covalent crosslinking, and potentially decrease required dosage of siRNA. Poly(kSer)/siRNA complexes showed no in vivo toxicity and demonstrated potential for efficient gene silencing. Future work will include an expanded in vivo study along with incorporation of disease models that will benefit from gene therapy. Overall, cross-linked poly(kSer)/siRNA complexes formulated via solvent-driven self-assembly demonstrate a new and feasible strategy for tackling multiple hurdles in siRNA delivery for safe RNAi therapy.

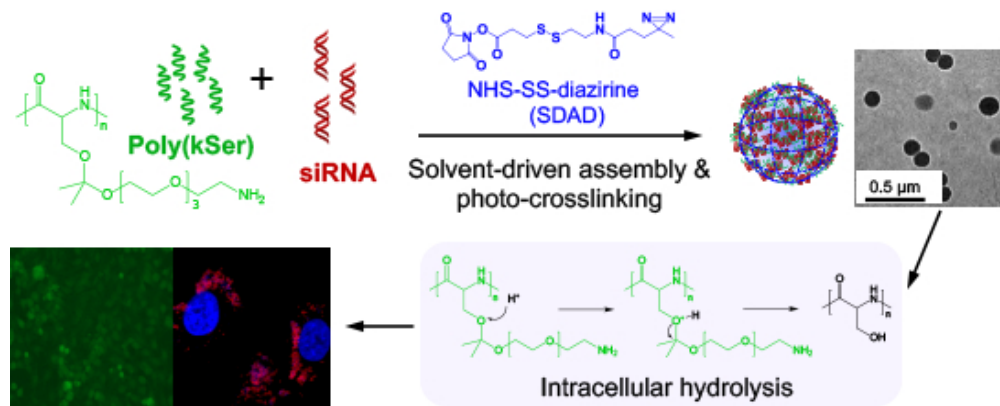## Conflicts of interest

There are no conflicts to declare.

Acknowledgements

Notes and references

1. B. Hu, Y. Weng, X. H. Xia, X. j. Liang and Y. Huang, *The journal of gene medicine*, 2019, **21**, e3097.
2. J. A. Kulkarni, D. Witzigmann, S. Chen, P. R. Cullis and R. van der Meel, *Accounts of chemical research*, 2019, **52**, 2435-2444.
3. A. E. Nel, L. Mädler, D. Velegol, T. Xia, E. M. Hoek, P. Somasundaran, F. Klaessig, V. Castranova and M. Thompson, *Nature materials*, 2009, **8**, 543-557.
4. R. L. Setten, J. J. Rossi and S.-p. Han, *Nature Reviews Drug Discovery*, 2019, **18**, 421-446.
5. M. Nakamori, E. Junn, H. Mochizuki and M. M. Mouradian, *Neurotherapeutics*, 2019, **16**, 287-298.
6. M. Zhu, L. Jiang, Y. Yuan, L. Chen, X. Liu, J. Liang, Q. Zhu, D. Ding and E. Song, *Cell and tissue research*, 2019, **376**, 341-351.
7. B. Kim, J. H. Park and M. J. Sailor, *Advanced Materials*, 2019, **31**, 1903637.
8. M. A. Subhan and V. Torchilin, *Translational Research*, 2019, **214**, 62-91.
9. C. Xu, D. Li, Z. Cao, M. Xiong, X. Yang and J. Wang, *Nano letters*, 2019, **19**, 2688-2693.
10. F. Wang, L. Gao, L.-Y. Meng, J.-M. Xie, J.-W. Xiong and Y. Luo, *ACS Applied Materials & Interfaces*, 2016, **8**, 33529-33538.
11. H. Lv, S. Zhang, B. Wang, S. Cui and J. Yan, *Journal of Controlled Release*, 2006, **114**, 100-109.

12. I. Lynch and K. A. Dawson, *Nano today*, 2008, **3**, 40-47.

13. J. Li, X. Yu, Y. Wang, Y. Yuan, H. Xiao, D. Cheng and X. Shuai, *Advanced Materials*, 2014, **26**, 8217-8224.

14. S. Itakura, S. Hama, R. Matsui and K. Kogure, *Nanoscale*, 2016, **8**, 10649-10658.

15. C. Zheng, M. Zheng, P. Gong, J. Deng, H. Yi, P. Zhang, Y. Zhang, P. Liu, Y. Ma and L. Cai, *Biomaterials*, 2013, **34**, 3431-3438.

16. Z.-X. Zhao, S.-Y. Gao, J.-C. Wang, C.-J. Chen, E.-Y. Zhao, W.-J. Hou, Q. Feng, L.-Y. Gao, X.-Y. Liu and L.-R. Zhang, *Biomaterials*, 2012, **33**, 6793-6807.

17. W. Tai and X. Gao, *Advanced drug delivery reviews*, 2017, **110**, 157-168.

18. R. H. Mo, J. L. Zaro and W.-C. Shen, *Molecular pharmaceutics*, 2012, **9**, 299-309.

19. D. J. Gary, J. Min, Y. Kim, K. Park and Y. Y. Won, *Macromolecular bioscience*, 2013, **13**, 1059-1071.

20. M. K. Brenner and M.-c. Hung, *Cancer Gene Therapy by Viral and Non-viral Vectors*, Wiley Online Library, 2014.

21. K. L. Kozielski, S. Y. Tzeng, B. A. Hurtado De Mendoza and J. J. Green, *ACS nano*, 2014, **8**, 3232-3241.

22. M. S. Shim and Y. J. Kwon, *Biomaterials*, 2010, **31**, 3404-3413.

23. L. Peng and E. Wagner, *Biomacromolecules*, 2019, **20**, 3613-3626.

24. S. Eskandari, T. Guerin, I. Toth and R. J. Stephenson, *Advanced Drug Delivery Reviews*, 2017, **110**, 169-187.

25. S. I. Lim, C. I. Lukianov and J. A. Champion, *Journal of Controlled Release*, 2017, **249**, 1-10.

26. X. Chen, J. Yang, H. Liang, Q. Jiang, B. Ke and Y. Nie, *Journal of Materials Chemistry B*, 2017, **5**, 1482-1497.

27. J.-A. Chuah, A. Matsugami, F. Hayashi and K. Numata, *Biomacromolecules*, 2016, **17**, 3547-3557.

28. D. M. Packwood, P. Han and T. Hitosugi, *Nature communications*, 2017, **8**, 1-8.

29. G. M. Whitesides and B. Grzybowski, *Science*, 2002, **295**, 2418-2421.

30. M. Li, M. Ehlers, S. Schlesiger, E. Zellermann, S. K. Knauer and C. Schmuck, *Angewandte Chemie International Edition*, 2016, **55**, 598-601.

31. S. Kumar, A. Pearse, Y. Liu and R. E. Taylor, *Nature Communications*, 2020, **11**, 2960.

32. L. Wang, C. Gong, X. Yuan and G. Wei, *Nanomaterials*, 2019, **9**, 285.

33. R. Jain and S. Roy, *Materials Science and Engineering: C*, 2020, **108**, 110483.

34. S. Wong and Y. J. Kwon, *Journal of Polymer Science Part A: Polymer Chemistry*, 2015, **53**, 280-286.

35. J. Wang, K. Liu, R. Xing and X. Yan, *Chemical Society Reviews*, 2016, **45**, 5589-5604.

36. L. Liu, K. Busuttil, S. Zhang, Y. Yang, C. Wang, F. Besenbacher and M. Dong, *Physical Chemistry Chemical Physics*, 2011, **13**, 17435-17444.

37. J. Wang, K. Liu, L. Yan, A. Wang, S. Bai and X. Yan, *ACS nano*, 2016, **10**, 2138-2143.

38. A. Wang, L. Cui, S. Debnath, Q. Dong, X. Yan, X. Zhang, R. V. Ulijn and S. Bai, *ACS Applied Materials & Interfaces*, 2017, **9**, 21390-21396.

39. Z. A. Arnon, A. Vitalis, A. Levin, T. C. Michaels, A. Caflisch, T. P. Knowles, L. Adler-Abramovich and E. Gazit, *Nature communications*, 2016, **7**, 1-7.

40. D. Punihaole, R. S. Jakubek, R. J. Workman, L. E. Marbella, P. Campbell, J. D. Madura and S. A. Asher, *The Journal of Physical Chemistry B*, 2017, **121**, 5953-5967.

41. K. Gekko, E. Ohmae, K. Kameyama and T. Takagi, *Biochimica et Biophysica Acta (BBA) - Protein Structure and Molecular Enzymology*, 1998, **1387**, 195-205.

42. J. Wu, W. Qu, J.-M. Williford, Y. Ren, X. Jiang, X. Jiang, D. Pan, H.-Q. Mao and E. Luijten, *Nanotechnology*, 2017, **28**, 204002.

43. B. Bozdoğan, Ö. Akbal, E. Çelik, M. Türk and E. B. Denkbaş, *RSC advances*, 2017, **7**, 47592-47601.

44. N. M. Correa, J. J. Silber, R. E. Riter and N. E. Levinger, *Chemical Reviews*, 2012, **112**, 4569-4602.

45. D. Han, X. Tong and Y. Zhao, *Langmuir*, 2012, **28**, 2327-2331.

46. Y. J. Kwon, *Accounts of chemical research*, 2012, **45**, 1077-1088.

47. C. He, H. Yue, L. Xu, Y. Liu, Y. Song, C. Tang and C. Yin, *Acta Biomaterialia*, 2020, **103**, 213-222.

48. J. Sankaranarayanan, E. A. Mahmoud, G. Kim, J. M. Morachis and A. Almutairi, *Acs Nano*, 2010, **4**, 5930-5936.

49. K. Raemdonck, R. E. Vandenbroucke, J. Demeester, N. N. Sanders and S. C. De Smedt, *Drug discovery today*, 2008, **13**, 917-931.

50. C. Coralli, M. Cemazar, C. Kanthou, G. M. Tozer and G. U. Dachs, *Cancer research*, 2001, **61**, 4784-4790.

46x18mm (300 x 300 DPI)